Local density of states of quasiparticles near the interface of nonuniform d-wave superconductors

Yukio Tanaka

Graduate School of Science and Technology and Department of Physics, Faculty of Science, Niigata University,
Ikarashi, Niigata 950-21, Japan

Satoshi Kashiwaya

Electrotechnical Laboratory, Tsukuba, Ibaraki 305, Japan

The local density of states of quasiparticle (LDOS) near the interface of d-wave superconductors is investigated for various situations based on the Green's-function method of nonuniform superconductors. In the case of normal-metal–insulator–d-wave-superconductor junction, the LDOS near the interface of the superconductor strongly depends on the angle between the normal to the interface and the crystalline axes of d-wave superconductor, on the thickness and on the height of the insulating barrier. In the case of d-wave-superconductor–insulator–d-wave-superconductor junction, bound states are formed at the interfaces of superconductors. The energy levels of bound states which include several limiting cases are explicitly obtained. The LDOS near the interface of the superconductor is strongly influenced by the bound states and it depends not only on the angle between the crystalline axes and the normal to the interface but also on the macroscopic phase difference between two superconductors.

I. INTRODUCTION

Energy spectrum of quasiparticles in nonuniform superconductors is one of the basic problems of superconductivity.[1] Nonuniformity induces the interference of the quasiparticles which can not be expected in the bulk systems. In general, two kinds of reflection process occur at the superconductor–normal-metal (S/N) interface. An electronlike quasiparticle injected from the $N(S)$ side is reflected as both an electronlike quasiparticle, which we will call normal reflection hereafter, and a holelike quasiparticle. The latter process originates from the existence of finite amplitude of the pair potential $\Delta(x)$ and is called the Andreev reflection.[2] In general, the local density of states of the quasiparticles (LDOS) in the nonuniform superconductor is influenced by the interference of these two kinds of quasiparticles. Previously there have been many theoretical studies on nonuniform superconductors.[3–11] However, except for a few cases of heavy fermion superconductors,[12–14] most theories have dealt with isotropic s-wave superconductors. Nowadays, symmetry of the pair potential of high-T_c superconductors has attracted attention,[15–17] and several groups have proposed d-wave symmetry for this.[18–21] Different from s-wave superconductors, the nature of quasiparticles near the interface of a d-wave superconductor is not fully clarified yet. In the d-wave superconductors, the quasiparticles experience different pair potentials depending on the direction of motion, and at the interface interference effects of quasiparticles, which are absent in the s-wave superconductors, are expected.

Recently, we developed a tunneling theory for a normal-metal–insulator–d-wave-superconductor ($N/I/d$) junction.[22] It was revealed that tunneling conductance spectra strongly depend on tunneling direction relative to crystalline axes and do not always represent the bulk density of states, in contrast to those of s-wave superconductors. In the $d_{x^2-y^2}$-wave su-

perconductors, since the pair potential changes its sign on the Fermi surface, the transmitted electronlike quasiparticle and the holelike quasiparticle feel different signs of the pair potential in the ab-plane junction. In such a case, quasiparticles with zero energy injected from the normal metal do not experience the insulating barrier due to the zero-energy states (ZES) which are formed near the interface of superconductor side. For this reason, tunneling conductance has peaks at zero energy. In light of our theory,[22] qualitative features of tunneling experiments in high-T_c superconductors are well understood with the d-wave symmetry of pair potentials.[23–26] If the magnitude of the height or thickness of the insulating barrier becomes infinite, the ZES become the bound states of the quasiparticle.[27–30] The origin of this bound states are discussed by Kashiwaya *et al.*,[31] in terms of quantized levels in a potential well of pair potentials.

Although, there have been several investigations treating the surface and interface of d-wave superconductors, quasiparticle states near the interface of d-wave superconductors are not fully investigated. The LDOS is obtained explicitly only in the d-wave superconductors[27–30] having semi-infinite or finite thickness. The aim of this paper is to elucidate what is expected in LDOS near the interface of d-wave superconductors in more general cases.

In this paper, we will investigate general cases with a Green's-function method in nonuniform d-wave superconductors based on a microscopic wave functions. Using the Green's function, quasiparticle states of d-wave superconductors near the interface of $N/I/d$ junctions will be studied by changing various parameters which characterize the orientation of the junction and the height or thickness of the barrier. We will also discuss the basic properties of d-wave superconductor–insulator–d-wave superconductor ($d/I/d$) junctions. It is known that bound states which are formed near the interface of s-wave superconductor–insulator–s-wave-superconductor ($s/I/s$) junctions strongly influence the Josephson current.[11] To elucidate the microscopic origin of the Josephson current, we must clarify the bound states in
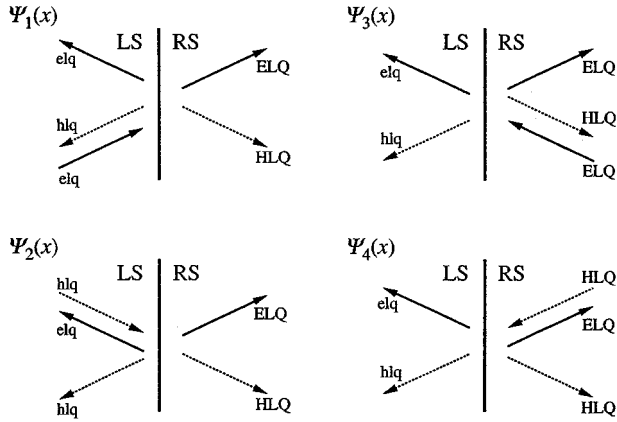
FIG. 1. Schematic illustration of the four types of reflection and transmission processes at the interface of wave functions $\Psi_l(x)$ ($l=1,4$). (a) $\Psi_1(x)$, (b) $\Psi_2(x)$, (c) $\Psi_3(x)$, and (d) $\Psi_4(x)$. In this figure, LS (RS), elq (ELQ), and hlq (HLQ) express left (right) superconductor, electronlike quasiparticle in left (right) superconductor and holelike quasiparticle in left (right) superconductor.

$d/I/d$ junctions. We will discuss how bound states at the interface depend on the angle between the crystalline axes and the normal to the interface and on the macroscopic phase difference between two superconductors. The organization of this paper is as follows. In Sec. II, the model and the method to calculate the Green's function in a nonuniform system is given. We have extended the previous theory of the Green's function by Furusaki and Tsukada in a one-dimensional s-wave superconductor[11] to singlet anisotropic superconductors. In Sec. III, the LDOS near the interface of the $N/I/d$ junction is investigated. We will also compare the LDOS with our previous results of the tunneling conductance. In Sec. IV, the LDOS of $d/I/d$ junctions is investigated. It will be clarified that the LDOS near the interface of the d-wave superconductor depends not only on the angle between the crystalline axes and the normal to the interface but also on the macroscopic phase difference between two superconductors. The relevance between the bound states and the LDOS is discussed in detail. Effects which are peculiar to $d/I/d$ junctions will be clarified. In Sec. V, we summarize our results and the future problems.

II. MODEL AND FORMULATION

For the simplest model calculation, we consider a two-dimensional anisotropic singlet superconductor–insulator–anisotropic singlet superconductor junction with perfectly flat interfaces in the clean limit. In this model, the interface is perpendicular to the x axis and is located at $x=0$ and $x=d$, where d is the thickness of insulating region. The Fermi wave number k_F and the effective mass m are assumed to be equal both in the left and right superconductor. Quasiparticle states in inhomogeneous anisotropic singlet superconductors can be described by the Bogoliubov–de Gennes equations[13,30]

$$Eu(\mathbf{x}_1)=h_0 u(\mathbf{x}_1)+\int d\mathbf{x}_2\, \Delta(\mathbf{s},\mathbf{r})v(\mathbf{x}_2),$$

$$Ev(\mathbf{x}_1)=-h_0 v(\mathbf{x}_1)+\int d\mathbf{x}_2\, \Delta^*(\mathbf{s},\mathbf{r})u(\mathbf{x}_2), \qquad (1)$$

where $\mathbf{s}=(\mathbf{x}_1-\mathbf{x}_2)$, $\mathbf{r}=(\mathbf{x}_1+\mathbf{x}_2)/2$, and $h_0=-\hbar^2\nabla^2_{\mathbf{x}_1}/2m+U(x)-\mu$, with μ the chemical potential. The energy of the quasiparticle E is measured from the Fermi energy $E_F(E_F=\mu)$. We can simply express Eq. (1) by the Nambu matrix formulation as

$$\int d\mathbf{x}_2 \vec{H}(\mathbf{x}_1,\mathbf{x}_2)\mathbf{\Psi}(\mathbf{x}_2)=\mathbf{\Psi}(\mathbf{x}_1), \quad \mathbf{\Psi}(\mathbf{x}_1)=\begin{pmatrix} u(\mathbf{x}_1) \\ v(\mathbf{x}_1) \end{pmatrix}. \tag{2}$$

We assume that the pair potential and Hartree potential are

$$\Delta(\mathbf{k},\mathbf{r})=\begin{cases} \Delta_L(\gamma)\exp(i\varphi_L), & x<0 \\ 0, & 0<x<d, \\ \Delta_R(\gamma)\exp(i\varphi_R), & x>d \end{cases} \tag{3}$$

$$U(x)=\begin{cases} 0, & x<0 \\ U_0, & 0<x<d \\ 0, & x>d, \end{cases}$$

where $\Delta(\mathbf{k},\mathbf{r})$ is the Fourier transform of $\Delta(\mathbf{s},\mathbf{r})$, with $\exp(i\gamma)\equiv k_x/|\mathbf{k}|+ik_y/|\mathbf{k}|$ using a wave vector $\mathbf{k}$. In the weak-coupling limit, $\mathbf{k}$ is fixed on the Fermi surface ($|\mathbf{k}|=k_F$).

The quantities φ_L and φ_R are the macroscopic phase of the left and right superconductor; respectively. The two component wave functions $\mathbf{\Psi}(\mathbf{x})$ satisfy following relations:

$$\mathbf{\Psi}(\mathbf{x})\big|_{x=0_-}=\mathbf{\Psi}(\mathbf{x})\big|_{x=0_+}, \quad \frac{d\mathbf{\Psi}(\mathbf{x})}{dx}\bigg|_{x=0_-}=\frac{d\mathbf{\Psi}(\mathbf{x})}{dx}\bigg|_{x=0_+} \tag{4}$$

$$\mathbf{\Psi}(\mathbf{x})\big|_{x=d_-}=\mathbf{\Psi}(\mathbf{x})\big|_{x=d_+}, \quad \frac{d\mathbf{\Psi}(\mathbf{x})}{dx}\bigg|_{x=d_-}=\frac{d\mathbf{\Psi}(\mathbf{x})}{dx}\bigg|_{x=d_+}. \tag{5}$$

Since the translational invariance is satisfied, the momentum parallel to the interface $k_y=k_F\sin\gamma$ is conserved. For given k_y, we can make the Green's function of quasiparticles extending the method of one-dimensional s-wave superconductor by Furusaki and Tsukada.[11] In general, there are four kinds of effective pair potentials of quasiparticles for fixed γ. For an energy $E>\{\max[\Delta_R(\gamma_+),\Delta_R(\gamma_-),\Delta_L(\gamma_+),\Delta_L(\gamma_-)]\}$, with $\gamma_+=\gamma$ and $\gamma_-=\pi-\gamma$, there are four independent eigenfunctions corresponding to four types of boundary conditions shown in Fig. 1. Four types of wave functions $\mathbf{\Psi}_l(\mathbf{r})$, $l=1,4$, which satisfy Eq. (1) can be written as

$$\Psi_l(\mathbf{x}) = \exp(ik_F y \, \sin\gamma)\Psi_l(x,\gamma), \quad (l=1,4) \tag{6}$$

$$\Psi_1(x,\gamma) = \begin{cases} \psi_{\alpha,L}(x,\gamma) + a_1\psi_{\bar{\alpha},L}(x,\gamma) + b_1\psi_{\beta,L}(x,\gamma), & (x<0) \\ \psi_{1,I}(x,\gamma), & (0<x<d) \\ g_1\psi_{\alpha,R}(x,\gamma) + h_1\psi_{\bar{\beta},R}(x,\gamma), & (x>d), \end{cases} \tag{7}$$

$$\Psi_2(x,\gamma) = \begin{cases} \psi_{\bar{\beta},L}(x,\gamma) + a_2\psi_{\beta,L}(x,\gamma) + b_2\psi_{\bar{\alpha},L}(x,\gamma), & (x<0) \\ \psi_{2,I}(x,\gamma), & (0<x<d) \\ g_2\psi_{\bar{\beta},R}(x,\gamma) + h_2\psi_{\alpha,R}(x,\gamma), & (x>d), \end{cases} \tag{8}$$

$$\Psi_3(x,\gamma) = \begin{cases} g_3\psi_{\beta,L}(x,\gamma) + h_3\psi_{\bar{\alpha},L}(x,\gamma), & (x<0), \\ \psi_{3,I}(x,\gamma), & (0<x<d) \\ \psi_{\beta,R}(x,\gamma) + a_3\psi_{\bar{\beta},R}(x,\gamma) + b_3\psi_{\alpha,R}(x,\gamma), & (x>d), \end{cases} \tag{9}$$

$$\Psi_4(x,\gamma) = \begin{cases} g_4\psi_{\bar{\alpha},L}(x,\gamma) + h_4\psi_{\beta,L}(x,\gamma), & (x<0) \\ \psi_{4,I}(x,\gamma), & (0<x<d) \\ \psi_{\bar{\alpha},R}(x,\gamma) + a_4\psi_{\alpha,R}(x,\gamma) + b_4\psi_{\bar{\beta},R}(x,\gamma), & (x>d), \end{cases} \tag{10}$$

where j expresses the indices L and R, and wave functions $\psi_{\alpha,j}(x,\gamma)$, $\psi_{\bar{\alpha},j}(x,\gamma)$, $\psi_{\beta,j}(x,\gamma)$, $\psi_{\bar{\beta},j}(x,\gamma)$, and $\psi_{l,I}(x,\gamma)$ satisfy the following equations:

$$\begin{pmatrix} H_0 & |\Delta_j(\gamma_+)|\exp(i\phi_j) \\ |\Delta_j(\gamma_+)|\exp(-i\phi_j) & -H_0 \end{pmatrix} \psi_{\alpha,j}(x,\gamma)$$
$$= E\psi_{\alpha,j}(x,\gamma), \tag{11}$$

$$\begin{pmatrix} H_0 & |\Delta_j(\gamma_+)|\exp(i\phi_j) \\ |\Delta_j(\gamma_+)|\exp(-i\phi_j) & -H_0 \end{pmatrix} \psi_{\bar{\alpha},j}(x,\gamma)$$
$$= E\psi_{\bar{\alpha},j}(x,\gamma), \tag{12}$$

$$\begin{pmatrix} H_0 & |\Delta_j(\gamma_-)|\exp(i\tilde{\phi}_j) \\ |\Delta_j(\gamma_-)|\exp(-i\tilde{\phi}_j) & -H_0 \end{pmatrix} \psi_{\beta,j}(x,\gamma)$$
$$= E\psi_{\beta,j}(x,\gamma), \tag{13}$$

$$\begin{pmatrix} H_0 & |\Delta_j(\gamma_-)|\exp(i\tilde{\phi}_j) \\ |\Delta_j(\gamma_-)|\exp(-i\tilde{\phi}_j) & -H_0 \end{pmatrix} \psi_{\bar{\beta},j}(x,\gamma)$$
$$= E\psi_{\bar{\beta},j}(x,\gamma), \tag{14}$$

and

$$\begin{pmatrix} H_0+U(x) & 0 \\ 0 & -H_0-U(x) \end{pmatrix} \psi_{l,I}(x,\gamma) = E\psi_{l,I}(x,\gamma), \tag{15}$$

with

$$H_0 = -\frac{\hbar^2}{2m}\frac{d^2}{dx^2} - E_F\cos^2\gamma, \tag{16}$$

and

$$\exp(i\phi_j) = \frac{\Delta_j(\gamma_+)}{|\Delta_j(\gamma_+)|}\exp(i\varphi_j),$$

$$\exp(i\tilde{\phi}_j) = \frac{\Delta_j(\gamma_-)}{|\Delta_j(\gamma_-)|}\exp(i\varphi_j). \tag{17}$$

By solving the above equations, Eqs. (11)–(15), five kinds of wave functions are explicitly expressed as

$$\psi_{\alpha,j}(x,\gamma) = \begin{pmatrix} u_j\exp(i\phi_j/2) \\ v_j\exp(-i\phi_j/2) \end{pmatrix} \exp\left[i\left(k_F\cos\gamma \right.\right.$$
$$\left.\left. +\frac{m\Omega_{j,+}}{\hbar^2 k_F\cos\gamma}\right)x\right], \tag{18}$$

$$\psi_{\bar{\alpha},j}(x,\gamma) = \begin{pmatrix} v_j\exp(i\phi_j/2) \\ u_j\exp(-i\phi_j/2) \end{pmatrix} \exp\left[i\left(k_F\cos\gamma \right.\right.$$
$$\left.\left. -\frac{m\Omega_{j,+}}{\hbar^2 k_F\cos\gamma}\right)x\right], \tag{19}$$

$$\psi_{\beta,j}(x,\gamma) = \begin{pmatrix} \tilde{u}_j\exp(i\tilde{\phi}_j/2) \\ \tilde{v}_j\exp(-i\tilde{\phi}_j/2) \end{pmatrix} \exp\left[-i\left(k_F\cos\gamma \right.\right.$$
$$\left.\left. +\frac{m\Omega_{j,-}}{\hbar^2 k_F\cos\gamma}\right)x\right], \tag{20}$$

$$\psi_{\bar{\beta},j}(x,\gamma) = \begin{pmatrix} \tilde{v}_j\exp(i\tilde{\phi}_j/2) \\ \tilde{u}_j\exp(-i\tilde{\phi}_j/2) \end{pmatrix} \exp\left[-i\left(k_F\cos\gamma \right.\right.$$
$$\left.\left. -\frac{m\Omega_{j,-}}{\hbar^2 k_F\cos\gamma}\right)x\right], \tag{21}$$

$$\psi_{l,I}(x,\gamma) = \begin{pmatrix} c_l\exp(-\lambda x)+d_l\exp(\lambda x) \\ e_l\exp(-\lambda x)+f_l\exp(\lambda x) \end{pmatrix}, \quad (l=1,4), \tag{22}$$

with

$$u_j = \sqrt{\frac{1}{2}\left(1+\frac{\Omega_{j,+}}{E}\right)}, \quad v_j = \sqrt{\frac{1}{2}\left(1-\frac{\Omega_{j,+}}{E}\right)},$$

$$\tilde{u}_j = \sqrt{\frac{1}{2}\left(1+\frac{\Omega_{j,-}}{E}\right)}, \quad \tilde{v}_j = \sqrt{\frac{1}{2}\left(1-\frac{\Omega_{j,-}}{E}\right)}, \tag{23}$$

and

$$\Omega_{j,+} = \sqrt{E^2 - |\Delta_j(\gamma_+)|^2}, \quad \Omega_{j,-} = \sqrt{E^2 - |\Delta_j(\gamma_-)|^2},$$

$$\lambda = \sqrt{\frac{2mU_0}{\hbar^2} - k_F^2 \cos^2\gamma}. \tag{24}$$

Here, we have assumed the relation, $U_0, E_F \gg |\Omega_{j,\pm}|$. To calculate the Green's function, it is necessary to obtain another wave function $\hat{\mathbf{\Psi}}(\mathbf{x})$ which satisfies,

$$\int d\mathbf{x}_1 \ \hat{\mathbf{\Psi}}^t(\mathbf{x}_1) \overleftarrow{\hat{H}}(\mathbf{x}_1, \mathbf{x}_2) = \hat{\mathbf{\Psi}}^t(\mathbf{x}_2), \quad \hat{\mathbf{\Psi}}(\mathbf{x}_2) = \begin{pmatrix} \hat{u}(\mathbf{x}_2) \\ \hat{v}(\mathbf{x}_2), \end{pmatrix} \tag{25}$$

$$E\hat{u}(\mathbf{x}_2) = h_0 \hat{u}(\mathbf{x}_2) + \int d\mathbf{x}_1 \ \Delta^*(\mathbf{s}, \mathbf{r}) \hat{v}(\mathbf{x}_1),$$

$$E\hat{v}(\mathbf{x}_2) = -h_0 \hat{v}(\mathbf{x}_2) + \int d\mathbf{x}_1 \ \Delta(\mathbf{s}, \mathbf{r}) \hat{u}(\mathbf{x}_1). \tag{26}$$

$\hat{\mathbf{\Psi}}(\mathbf{x})$ also satisfies the boundary conditions given by Eqs. (3) and (4). For an energy $E > \{\max[\Delta_R(\gamma_+), \Delta_R(\gamma_-), \Delta_L(\gamma_+), \Delta_L(\gamma_-)]\}$, there are four independent eigenfunctions corresponding to four types of boundary conditions shown in Fig. 2. Four types of wave functions $\hat{\mathbf{\Psi}}_l(\mathbf{x})$ ($l = 1,4$), which satisfy Eq. (25) can be written as

$$\hat{\mathbf{\Psi}}_l(\mathbf{x}) = \exp(-ik_F y \ \sin\gamma) \hat{\Psi}_l(x, \gamma), \quad (l = 1,4). \tag{27}$$
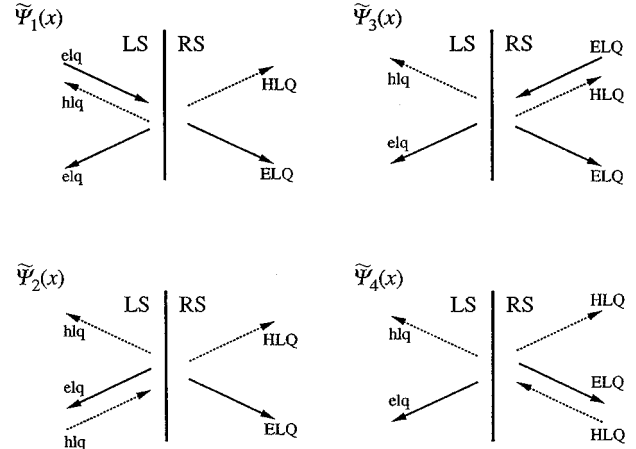
FIG. 2. Schematic illustration of the four types of reflection and transmission processes at the interface of wave functions $\hat{\mathbf{\Psi}}_l(\mathbf{x})$, ($l = 1,4$). (a) $\hat{\mathbf{\Psi}}_1(\mathbf{x})$, (b) $\hat{\mathbf{\Psi}}_2(\mathbf{x})$, (c) $\hat{\mathbf{\Psi}}_3(\mathbf{x})$, and (d) $\hat{\mathbf{\Psi}}_4(\mathbf{x})$. In this figure, LS (RS), elq (ELQ), and hlq (HLQ) express left (right) superconductor, electronlike quasiparticle in left (right) superconductor and holelike quasiparticle in left (right) superconductor.

The $\hat{\mathbf{\Psi}}_l(x, \gamma)$ are obtained from the $\Psi_l(x, \gamma)$ in Eqs. (7)–(10) by replacing all of the $\psi_{\delta,j}(x, \gamma)$ for $\delta = \alpha, \bar{\alpha}, \beta, \bar{\beta}, \psi_{j,I}(x, \gamma)$, $a_j, b_j, \ldots, g_j,$ and h_j by the analogous $\hat{\psi}_{\delta,j}(x, \gamma)$, $\hat{\psi}_{j,I}(x, \gamma)$, $\hat{a}_j$, etc. The $\hat{\psi}_{\delta,j}(x, \gamma)$ and $\hat{\psi}_{j,I}(x, \gamma)$ are obtained from Eqs. (11)–(15) by replacing the $\psi_{\delta,j}(x, \gamma)$, $\psi_{j,I}(x, \gamma)$ by $\hat{\psi}_{\delta,j}(x, \gamma)$ and $\hat{\psi}_{j,I}(x, \gamma)$, and by interchanging $\gamma_\pm$ with $\gamma_\mp$ and $\phi_j(\bar{\phi}_j)$ with $-\phi_j(-\bar{\phi}_j)$. The explicit forms for the $\hat{\psi}_{\delta,j}(x, \gamma)$ can be obtained from Eqs. (18)–(21) by interchanging u_j with $\tilde{u}_j$, v_j with $\tilde{v}_j$, and $\Omega_{j,+}$ with $\Omega_{j,-}$. $\hat{\psi}_{l,I}(x, \gamma)$ may be written analogously to Eq. (22), by replacing the coefficients c_l, etc., by $\hat{c}_l$, etc. We can make the Green's function as follows:

$$G^\tau(x, x', k_y, E) = \begin{cases} \alpha_1 \Psi_3(x, \gamma) \hat{\Psi}_1^t(x', \gamma) + \alpha_2 \Psi_3(x, \gamma) \hat{\Psi}_2^t(x', \gamma) + \alpha_3 \Psi_4(x, \gamma) \hat{\Psi}_1^t(x', \gamma) + \alpha_4 \Psi_4(x, \gamma) \hat{\Psi}_2^t(x', \gamma) & x < x' \\ \beta_1 \Psi_1(x, \gamma) \hat{\Psi}_3^t(x', \gamma) + \beta_2 \Psi_2(x, \gamma) \hat{\Psi}_3^t(x', \gamma) + \beta_3 \Psi_1(x, \gamma) \hat{\Psi}_4^t(x', \gamma) + \beta_4 \Psi_2(x, \gamma) \hat{\Psi}_4^t(x', \gamma) & x > x'. \end{cases} \tag{28}$$

Using the above functions, we can construct the Green's function as follows:

$$\int [E - \overrightarrow{H}(x, x'', k_y)] G^\tau(x'', x', k_y, E) dx''$$

$$= \delta(x - x') \begin{pmatrix} 1 & 0 \\ 0 & 1 \end{pmatrix}, \tag{29}$$

$$\int G^\tau(x, x'', k_y, E)[E - \overleftarrow{H}(x'', x', k_y)] dx''$$

$$= \delta(x - x') \begin{pmatrix} 1 & 0 \\ 0 & 1 \end{pmatrix}, \tag{30}$$

where $H(x, x'', k_y)$ is the Fourier transform with respect to $y - y''$ of $H(x, x'')$. The quantities α_i and β_i ($i = 1,4$) in Eq. (28) are determined so that $G^\tau(x, x', k_y, E)$ satisfy following equations:

$$\left.\frac{\partial}{\partial x} G^\tau(x, x', k_y, E)\right|_{x = x' + 0} - \left.\frac{\partial}{\partial x} G^\tau(x, x', k_y, E)\right|_{x = x' - 0}$$

$$= \frac{2m}{\hbar^2} \begin{pmatrix} 1 & 0 \\ 0 & -1 \end{pmatrix}, \tag{31}$$

$$G^\tau(x, x+0, k_y, E) = G^\tau(x, x-0, k_y, E). \tag{32}$$

The LDOS of the quasiparticle can be obtained as

$$\rho(E, x) = \sum_{k_y} \frac{-1}{\pi} \text{Im}[G_{11}^\tau(x, x, k_y, E)], \tag{33}$$

where $G_{11}^\tau(x, x, k_y, E)$ are the 11 component of a 2×2 retarded Green's function. In the following, we calculate the LDOS for several cases.

III. LDOS OF NORMAL-METAL−INSULATOR−d-WAVE-SUPERCONDUCTOR JUNCTIONS

In this section, we calculate the LDOS of normal-metal–insulator–d-wave-superconductor ($N/I/d$) junctions for several cases, where Hartree potential is expressed as a square as discussed in Sec. II. The LDOS of the quasiparticle which is normalized by those in the normal state is explicitly given as

$$\rho(E,x)=\mathrm{Re}\left\{\frac{1}{2\pi}\int_{-\pi/2}^{\pi/2}d\gamma[\rho_+(E,x,\gamma)+\rho_-(E,x,\gamma)]\right\},$$
(34)

with

$$\rho_\pm(E,x,\gamma)=\frac{1}{\Omega_{R,\pm}}\left\{E+|\Delta_R(\gamma_\pm)|F_\pm\exp\left[2i\frac{(x-d)}{\xi_\pm}\right]\right\},$$

$$\xi_\pm=\frac{\hbar^2 k_F\cos\gamma}{m\Omega_{R,\pm}}.$$
(35)

In the above, $F_\pm$ is given as

$$F_\pm=\frac{(1-\sigma_N)\Gamma_{R,\mp}\exp[i(\tilde{\phi}_R-\phi_R)]-\Gamma_{R,\pm}}{1-(1-\sigma_N)\Gamma_{R,\pm}\Gamma_{R,\mp}\exp[i(\tilde{\phi}_R-\phi_R)]},$$
(36)

using

$$\Gamma_{R,\pm}=\frac{|\Delta_R(\gamma_\pm)|}{E+\Omega_{R,\mp}},$$

$$\sigma_N=\frac{4Z_\gamma^2}{(1-Z_\gamma^2)^2\sinh^2(\lambda d)+4Z_\gamma^2\cosh^2(\lambda d)},$$

$$\lambda=(1-\kappa^2\cos^2\gamma)^{1/2}\lambda_0,$$
(37)

with

$$Z_\gamma=\frac{\kappa\cos\gamma}{\sqrt{1-\kappa^2\cos^2\gamma}},\quad \lambda_0=\sqrt{\frac{2mU_0}{\hbar^2}},\quad \kappa=\frac{k_F}{\lambda_0}.$$
(38)

In the above, σ_N expresses the tunneling conductance of the $N/I/d$ junction in the normal states which was defined in our previous papers.[22,27] The pair potentials $\Delta_R(\gamma_+)$ and $\Delta_R(\gamma_-)$ in Eqs. (17) and (24) are expressed as

$$\Delta_R(\gamma_+)=\Delta_0\cos[2(\gamma-\beta)],$$

$$\Delta_R(\gamma_-)=\Delta_0\cos[2(\gamma+\beta)],$$
(39)

where β stands for the angle between the crystalline axis of the right superconductor and the normal to the interface. In Eqs. (34) and (35), the atomic scale oscillations of $\rho(E,x)$ are averaged out. Within this approximation, $\rho(E,x)$ in the normal metal becomes 1 for any x. The drastic effect occurs when the signs of $\Delta_R(\gamma_+)$ and $\Delta_R(\gamma_-)$ are different from each other as we will see below.

In Fig. 3, $\rho(E,x)$ with $\beta=0$ is plotted for various λ_0 and κ. In the case of (a), since d is zero, $\rho(E,x)$ does not depend on λ_0 and κ. As shown by curve A, $\rho(E,x)$ at $x=d$ becomes
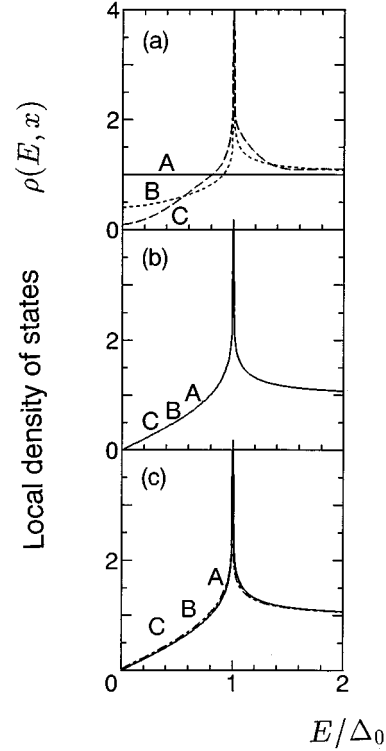
FIG. 3. Normalized local density of states $\rho(E,x)$ with $\beta=0$ is plotted for (a) $\lambda_0 d=0$, (b) $\lambda_0 d=3$, $\kappa=0.1$, and (c) $\lambda_0 d=3$, $\kappa=0.9$. A: $x=d$, B: $x=d+0.5\xi_0$, C: $x=d+2.5\xi_0$.

1 independent of E, which is the value of the normal state. However as x increases, $\rho(E,x)$ approaches that of bulk DOS of the d-wave superconductor. The characteristic length of the spatial dependence of $\rho(E,x)$ is $\xi_0=\hbar v_F/\Delta_0$. In the case of (b) and (c), $\rho(E,x)$ qualitatively coincides with the bulk DOS of the d-wave superconductor independent of x. In (b) and (c), since the magnitude of the height and the thickness of the barrier is sufficiently large ($\sigma_N\sim 0$), quasiparticles in the superconductor are not influenced by the adjacent normal metal. In Fig. 4, $\rho(E,x)$ with $\beta=\pi/4$ is plotted for various λ_0 and κ. In the case of (a), $\rho(E,x)$ at $x=d$ becomes 1 independent of E, and it approaches that of the bulk DOS of the d-wave superconductor with the increase of x as in the case of Fig. 3(a). However, if $\lambda_0 d$ becomes finite, as shown in Figs. 4(b) and 4(c), qualitative features of $\rho(E,x)$ are significantly changed. In both curves (b) and (c), $\rho(E,x)$ at $E=0$ is drastically enhanced. As compared to $\sigma(E)$ of Fig. 2 in,[22] when the insulating barrier is sufficiently high, E dependence of $\rho(E,d)$ is similar to that of $\sigma(E)$. It has been clarified recently, for $\sigma_N\rightarrow 0$, $\sigma(E)$ can be expressed by $\rho(E,d)$.[32] In the limit of $\lambda_0 d\rightarrow\infty$ ($\sigma_N\rightarrow 0$), the denominator of $F_\pm$ vanishes for $E=0$ and bound states are formed at this energy near the interface.[28–30]

Let us see how the width of this peak changes as the function of $\lambda_0 d$ and κ. In Fig. 5, $\rho(E,d)$ is plotted for various $\lambda_0 d$ with a fixed value of κ. The width of the peak becomes narrower as $\lambda_0 d$ increases. On the other hand, the width of the peak becomes narrower as κ decreases as seen in the plot of $\rho(E,d)$ for various κ with a fixed value of $\lambda_0 d$ (see Fig. 6). Taking into account the fact that the quantity κ decreases with the increase of the barrier height, it can be summarized that the width of the peak decreases with the increase of the
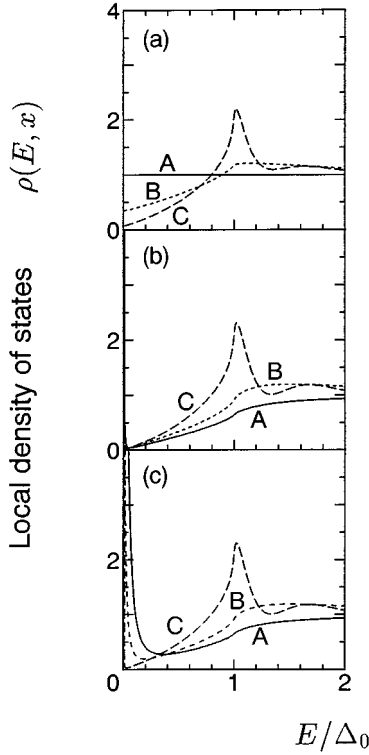
FIG. 4. Normalized local density of states $\rho(E,x)$ with $\beta=\pi/4$ is plotted for (a) $\lambda_0 d=0$, (b) $\lambda_0 d=3$, $\kappa=0.1$, and (c) $\lambda_0 d=3$, $\kappa=0.9$. A: $x=d$, B: $x=d+0.5\xi_0$, C: $x=d+2.5\xi_0$.

thickness and the height of the barrier. For the next step, we will discuss the magnitude of $\rho(0,x)$. In Fig. 7, β dependence of $\rho(0,d)$ is plotted. As a reference, $\rho(E=0.01\Delta_0, d)$ and $\rho(E=0.02\Delta_0,d)$ are also plotted. As seen from Fig. 7, $\rho(E,d)$ is drastically suppressed as E deviates from zero and $\rho(E,d)$ is strongly enhanced near $\beta=\pi/4$. The quantity $\rho(0,d)$ can be written as

$$\rho(0,d)=\mathrm{Re}\left[\frac{1}{\pi}\int_{-\pi/2}^{\pi/2}\left\{\frac{1-(1-\sigma_N)\exp[i(\tilde{\phi}_R-\phi_R)]}{1+(1-\sigma_N)\exp[i(\tilde{\phi}_R-\phi_R)]}\right\}d\gamma\right].\tag{40}$$
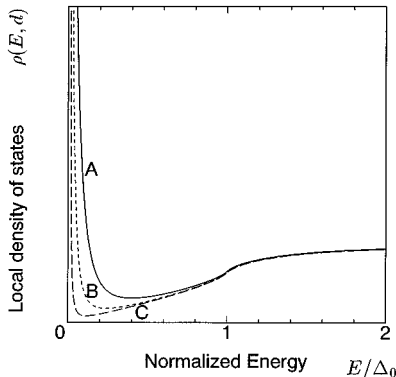
FIG. 5. Normalized local density of states at the interface $\rho(E,d)$ with $\beta=\pi/4$ and $\kappa=0.1$ is plotted for A: $\lambda_0 d=0.5$, B: $\lambda_0 d=1$, and C: $\lambda_0 d=2$.
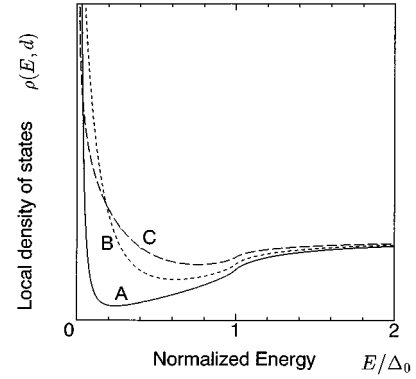
FIG. 6. Normalized local density of states at the interface $\rho(E,d)$ with $\beta=\pi/4$ with $\lambda_0 d=1$ is plotted for A: $\kappa=0.1$, B: $\kappa=0.5$, and C: $\kappa=0.9$.

For $\beta=\pi/4$, $\Delta_R(\gamma_+)\Delta_R(\gamma_-)<0$ and $\exp[i(\tilde{\phi}_R-\phi_R)]=-1$ are satisfied for any γ. In such a case, the integrand of Eq. (40) becomes $(2-\sigma_N)/\sigma_N$ and diverges for $\sigma_N\rightarrow0$ ($\lambda_0 d\rightarrow\infty$, $\kappa\rightarrow0$). If we use δ-function barrier model, the integral with the variable γ can be performed rigorously. Replacing σ_N in Eq. (40) by

$$\sigma_N=\frac{4\cos^2\theta}{4\cos^2\theta+Z^2},\quad Z=\frac{\lambda_0^2 d}{k_F},\tag{41}$$

we can reproduce the δ-function barrier model as discussed in our previous paper.[22,27] We can rigorously obtain $\rho(0,d)$ as

$$\rho(0,d)=[1-F(Z)]+\frac{2F(Z)}{\pi}\left\{\tan^{-1}\left[F(Z)\tan\left(\frac{\pi}{4}+\beta\right)\right]\right.$$
$$\left.-\tan^{-1}\left[F(Z)\tan\left(\frac{\pi}{4}-\beta\right)\right]\right\}+\frac{Z^2}{\pi}\left[\tan\left(\frac{\pi}{4}+\beta\right)\right.$$
$$\left.-\tan\left(\frac{\pi}{4}-\beta\right)\right],\tag{42}$$
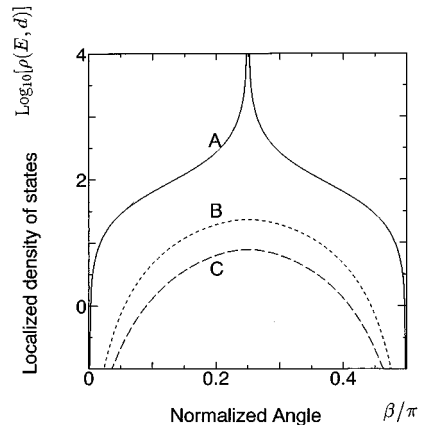
with

FIG. 7. Normalized local density of states at the interface $\rho(E,d)$ with $\lambda_0 d=1$ and $\kappa=0.1$ is plotted as a function of β for A: $E=0$, B: $E=0.01\Delta_0$, and C: $E=0.02\Delta_0$.
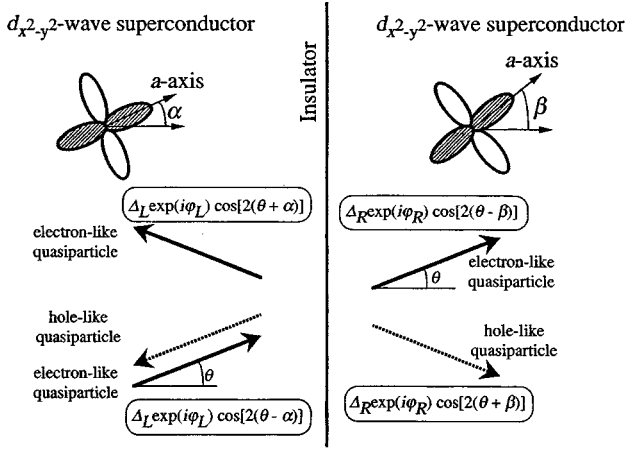
FIG. 8. Schematic illustration of the reflection and transmission processes at the interface. In this figure, the quantities θ and $\alpha(\beta)$ express the injection angle of the electron and the angle between the normal vector of the interface and the a axis of the left (right) $d_{x^2-y^2}$-wave superconductor, respectively. $\Delta_R = \Delta_L = \Delta_0$.

$$F(Z) = \frac{Z}{\sqrt{Z^2 + 2}}. \tag{43}$$

The divergence of $\rho(0,d)$ at $\beta = \pi/4$ is obtained for $Z \neq 0$.

IV. LDOS OF d-WAVE SUPERCONDUCTOR– INSULATOR–d-WAVE-SUPERCONDUCTOR JUNCTIONS

In this section, the LDOS of the d-wave superconductor–insulator–d-wave-superconductor ($d/I/d$) junction is discussed for various crystal angle rotations α and β. The macroscopic phase difference $\varphi = \varphi_R - \varphi_L$ is measured along the a axis as shown in Fig. 8. If the electronlike quasiparticle is injected from the left superconductor, the incidental electronlike quasiparticle and the reflected electronlike quasiparticle feel different effective pair potentials for $\alpha \neq 0$. As in the left superconductor, the transmitted electronlike quasiparticle and the holelike quasiparticle feel the different pair potentials for $\beta \neq 0$. In general, there are four kinds of effective pair potentials of quasiparticles for fixed θ. The bound states are formed near the interface when the energy of the quasiparticle E satisfies $E \leqslant \min[\Delta_L(\theta_+), \Delta_L(\theta_-), \Delta_R(\theta_+), \Delta_R(\theta_-)]$, where the effective pair potentials in the left superconductor $\Delta_L(\theta_+)$ and $\Delta_L(\theta_-)$ are expressed as

$$\Delta_L(\theta_+) = \Delta_0 \cos[2(\theta - \alpha)], \quad \Delta_L(\theta_-) = \Delta_0 \cos[2(\theta + \alpha)], \tag{44}$$

and those of in the right superconductor $\Delta_R(\theta_+)$ and $\Delta_R(\theta_-)$ are expressed as

$$\Delta_R(\theta_+) = \Delta_0 \cos[2(\theta - \beta)],$$

$$\Delta_R(\theta_-) = \Delta_0 \cos[2(\theta + \beta)]. \tag{45}$$

The energy levels of the bound states are written as

$$(1-\sigma_N)\{\gamma_1\gamma_2 - \exp[i(\theta_1+\theta_2)]\}\{\gamma_3\gamma_4 - \exp[i(\theta_3+\theta_4)]\}$$

$$+ \sigma_N\{\gamma_1\gamma_3 - \exp[i(\theta_1+\theta_3+\varphi)]\}\{\gamma_2\gamma_4 - \exp[i(\theta_2$$

$$+ \theta_4 - \varphi)]\} = 0, \tag{46}$$

where

$$\theta_1 = \arctan(\sqrt{|\Delta_L(\theta_+)|^2 - E^2}/E),$$

$$\theta_2 = \arctan(\sqrt{|\Delta_L(\theta_-)|^2 - E^2}/E),$$

$$\theta_3 = \arctan(\sqrt{|\Delta_R(\theta_+)|^2 - E^2}/E),$$

$$\theta_4 = \arctan(\sqrt{|\Delta_R(\theta_-)|^2 - E^2}/E). \tag{47}$$

The quantities γ_i ($i = 1,4$) are expressed as

$$\gamma_1 = \frac{\Delta_L(\theta_+)}{|\Delta_L(\theta_+)|}, \quad \gamma_2 = \frac{|\Delta_L(\theta_-)|}{\Delta_L(\theta_-)}, \quad \gamma_3 = \frac{|\Delta_R(\theta_+)|}{\Delta_R(\theta_+)},$$

$$\gamma_4 = \frac{\Delta_R(\theta_-)}{|\Delta_R(\theta_-)|}. \tag{48}$$

Equation (46) is the generalized version of the quantized condition of bound states of quasiparticles in $s/I/s$ junctions.[31] In the case of $\sigma_N = 0$, bound states are determined independently in the left and the right superconductors, and this condition corresponds to that of the semi-infinite superconductors.[27,28–31] In the other limiting case, $\sigma_N = 1$, only Andreev reflection exists and θ_+ and θ_- can be treated separately. In the following, we will pay attention to the θ dependence of the energy level of bound state (E_b) whose energy is positive. We can expect the same magnitude of E_b in the negative energy region since time-reversal symmetry is not broken. In the case of the $s/I/s$ junction, the above bound-states condition is reduced to[4,5,7,8]

$$E_b = \Delta_0 \sqrt{\cos^2\left(\frac{\varphi}{2}\right) + (1-\sigma_N)\sin^2(\varphi/2)}. \tag{49}$$

In the case of $\lambda_0 d = 0$, i.e., $\sigma_N = 1$, E_b depends on φ significantly, while for $\lambda_0 d \to \infty$, i.e., $\sigma_N \to 0$, E_b converges to Δ_0 independent of φ. The existence of the normal reflection reduces σ_N and strongly influences the energy levels.[11] In the case of $d/I/d$ junctions, we can express the energy levels of bound states simply for several cases. For $\alpha = \beta = 0$, E_b is expressed as

$$E_b = \Delta_0 |\cos(2\theta)| \sqrt{\cos^2(\varphi/2) + (1-\sigma_N)\sin^2(\varphi/2)}. \tag{50}$$

In this case, since $\Delta_L(\theta_+) = \Delta_L(\theta_-)$ and $\Delta_R(\theta_+) = \Delta_R(\theta_-)$ are satisfied, the effective pair potentials for the quasiparticle do not change at the normal reflection process at the interface in each superconductor. This is the reason why Eq. (50) is similar to Eq. (49) except for the factor $\cos(2\theta)$. The θ dependence of E_b is plotted in Figs. 9(a) and 9(b). The zero-energy states (ZES) for $\varphi = \pi$ in (a) disappear in (b) as in the case of s-wave superconductor. In the case of $\alpha = \beta = \pi/4$, θ dependence of E_b is expressed as

$$E_b = \Delta_0 |\sin(2\theta)| \cos(\varphi/2) \sqrt{\sigma_N}, \tag{51}$$

and is plotted in Figs. 10(a) and 10(b). When normal reflection is absent ($\sigma_N = 1$) as in (a), E_b is obtained by substituting $|\sin(2\theta)|$ for $|\cos(2\theta)|$ in Eq. (50). While in the case of (b) ($\sigma_N \neq 1$), the effective pair potentials for quasiparticles change their sign at the normal reflection at the interface. In this case, for $\sigma_N \to 0$, E_b approaches zero for every φ. The
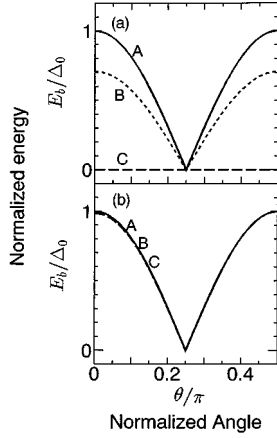
FIG. 9. The bound state energy E_b is plotted as a function of θ for a $d/I/d$ junction for $\alpha=0$ and $\beta=0$ with A: $\varphi=0$, B: $\varphi=\pi/2$ and C: $\varphi=\pi$. (a) $\lambda_0 d=0$, (b) $\lambda_0 d=1$, $\kappa=0.1$.

origin of the ZES is similar to that of the ZES at the interface of the $N/I/d$ junction or surface of the d-wave superconductor as discussed in the previous section.[26–32] In general, θ dependence of E_b becomes very complex.

Applying the Green's-function method discussed in Sec. II, the LDOS can be expressed as

$$\rho(x,E)=\mathrm{Re}\left\{\frac{1}{2\pi}\int_{-\pi/2}^{\pi/2}\left[\frac{E}{\Omega_{L,+}}+\Gamma\frac{|\Delta_{L,+}|}{\Omega_{L,+}}\exp\left(\frac{2x}{\xi_+}\right)\right.\right.$$
$$\left.\left.+\frac{E}{\Omega_{L,-}}+\tilde{\Gamma}\frac{|\Delta_{L,-}|}{\Omega_{L,-}}\exp\left(\frac{2x}{\xi_-}\right)\right]d\gamma\right\},\quad(x<0).$$
$$(52)$$

In the above, Γ and $\bar{\Gamma}$ are expressed as

$$\Gamma=-\frac{\Gamma_A\Gamma_B(1-\sigma_N)+\sigma_N\Gamma_C\Gamma_D}{\Gamma_A\Gamma_E(1-\sigma_N)+\sigma_N\Gamma_C\Gamma_F},\qquad(53)$$
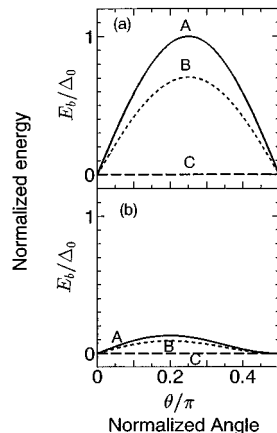
FIG. 10. The bound-state energy E_b is plotted as a function of θ for a $d/I/d$ junction for $\alpha=\pi/4$ and $\beta=\pi/4$ with A: $\varphi=0$, B: $\varphi=\pi/2$ and C: $\varphi=\pi$. (a) $\lambda_0 d=0$, (b) $\lambda_0 d=1$, $\kappa=0.1$.
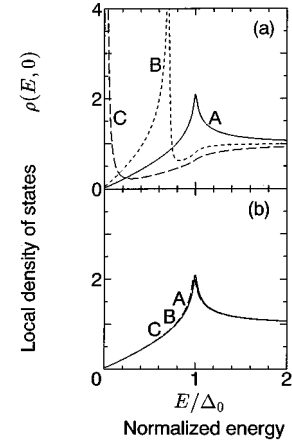
FIG. 11. Normalized local density of states $\rho(E,0)$ is calculated for $\alpha=0$ and $\beta=0$, with A: $\varphi=0$, B: $\varphi=\pi/2$ and C: $\varphi=\pi$. (a) $\lambda_0 d=0$, (b) $\lambda_0 d=1$, $\kappa=0.1$.

$$\tilde{\Gamma}=-\frac{\tilde{\Gamma}_A\tilde{\Gamma}_B(1-\sigma_N)+\sigma_N\tilde{\Gamma}_C\tilde{\Gamma}_D}{\tilde{\Gamma}_A\tilde{\Gamma}_E(1-\sigma_N)+\sigma_N\tilde{\Gamma}_C\tilde{\Gamma}_F},$$

with

$$\Gamma_A=1-\Gamma_{R,+}\Gamma_{R,-}-\gamma_3\gamma_4,\quad\Gamma_B=\Gamma_{L,+}-\Gamma_{L,-}-\gamma_1\gamma_2,$$

$$\Gamma_C=1-\Gamma_{L,-}\Gamma_{R,-}-\gamma_2\gamma_4\exp(i\varphi),$$

$$\Gamma_D=\Gamma_{L,+}-\Gamma_{R,+}-\gamma_1\gamma_3\exp(-i\varphi),\qquad(54)$$

$$\Gamma_E=1-\Gamma_{L,+}\Gamma_{L,-}-\gamma_1\gamma_2,$$

$$\Gamma_F=1-\Gamma_{L,+}\Gamma_{R,+}-\gamma_1\gamma_3\exp(-i\varphi),$$

and

$$\tilde{\Gamma}_A=\Gamma_A,\quad\tilde{\Gamma}_B=\Gamma_{L,-}-\Gamma_{L,+}-\gamma_1\gamma_2,\quad\tilde{\Gamma}_C=\Gamma_F,$$
$$(55)$$
$$\tilde{\Gamma}_D=\Gamma_{L,-}-\Gamma_{R,-}-\gamma_2\gamma_4\exp(i\varphi),\quad\tilde{\Gamma}_E=\Gamma_E,\quad\tilde{\Gamma}_F=\Gamma_C.$$

In the above $\Gamma_{L,\pm}$ and $\Gamma_{R,\pm}$ are given as

$$\Gamma_{L,\pm}=\frac{|\Delta_L(\gamma_\pm)|}{E+\Omega_{L,\pm}},\quad\Gamma_{R,\pm}=\frac{|\Delta_R(\gamma_\pm)|}{E+\Omega_{R,\pm}}.\qquad(56)$$

The denominators of Γ and $\tilde{\Gamma}$ vanish when E coincides with E_b for given γ. Equation (52) is the generalized expressions of the LDOS of the $d/I/d$ junction. For $\sigma_N=0$, we can reproduce the previous results of the LDOS in the semi-infinite superconductor.[28,30] In the following, to see the feature of the bound states, the quasiparticle energy E is substituted for $E+i\delta$, where δ is chosen as $0.01\Delta_0$. However the essence of the physics is not changed by the introduction of δ. In Figs. 11 and 12, the LDOS at $x=0$ is plotted for various α, β, and
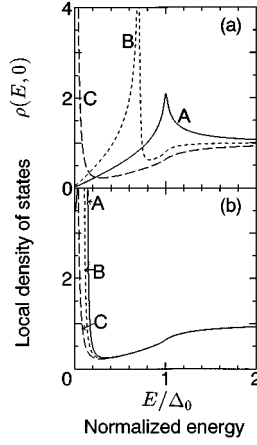
FIG. 12. Normalized local density of states $\rho(E,0)$ is calculated for $\alpha=\pi/4$ and $\beta=\pi/4$ with A: $\varphi=0$, B: $\varphi=\pi/2$ and C: $\varphi=\pi$. (a) $\lambda_0 d=0$, (b) $\lambda_0 d=1$, $\kappa=0.1$.

φ. In the case of (a), $\lambda_0 d$ is chosen as 0 ($\sigma_N=1$) and only the Andreev reflection occurs. On the other hand, in the case of (b), both the Andreev and the normal reflections occur, since $\lambda_0 d=1$ and $\kappa=0.1$ ($\sigma_N \neq 1$) are satisfied. In Fig. 11, several parameters are chosen as the same as those of Fig. 9. In every curve of the LDOS the position of peaks corresponds to the energy where E_b has maxima as a function of γ. This fact also holds in Fig. 12, where the same parameters are chosen as those in Fig. 10. Under the existence of $E_b=0$ for any γ, $\rho(E,0)$ has maximum at $E=0$. In the following, let us discuss the zero-energy level of bound states and $\rho(0,0)$. For $E=0$, Eq. (46) is transformed into

$$(1+\gamma_1\gamma_2)(1+\gamma_3\gamma_4)(1-\sigma_N)+\sigma_N[\gamma_1\gamma_3+\exp(i\varphi)]$$

$$\times[\gamma_2\gamma_4+\exp(-i\varphi)]=0. \qquad (57)$$

In d-wave superconductors, since $\gamma_i=\pm 1$ ($i=1,4$) are satisfied in general, bound states are formed only when $\varphi=0$ or $\varphi=\pi$. For $\sigma_N=1$, Eq. (57) is more simplified as

$$[\gamma_1\gamma_3+\exp(i\varphi)][\gamma_2\gamma_4+\exp(-i\varphi)]=0. \qquad (58)$$

In the cases of Figs. 11 and 12, $\gamma_1\gamma_3=\gamma_2\gamma_4=1$ is satisfied for any γ, and the ZES are only expected for $\varphi=\pi$. However as shown in Fig. 13(a), where $\alpha=\pi/4$ and $\beta=0$ are satisfied, $\gamma_1\gamma_3$ and $\gamma_2\gamma_4$ have different signs and the ZES are also expected for $\varphi=0$. While in the limit of $\lambda_0 d\rightarrow\infty$ or $\kappa\rightarrow 0$, ($\sigma_N\rightarrow 0$), Eq. (46) can be transformed into

$$(\gamma_1\gamma_2+1)(\gamma_3\gamma_4+1)=0. \qquad (59)$$

As seen from this equation, the condition whether the ZES are formed or not does not depend on φ at all. We can also see this tendency for $\sigma_N\sim 0$ shown in Figs. 11(b), 12(b), and 13(b), where the φ dependence of $\rho(0,0)$ is weak.

In the following, we will see how the ZES are influenced by φ for various α and β. Hereafter, we will define $\rho_0(\varphi,\alpha,\beta)\equiv\rho(0,0)$ with $\pi/4>\alpha,\beta>-\pi/4$. The quantity $\rho_0(\varphi,\alpha,\beta)\equiv\rho(0,0)$ satisfies
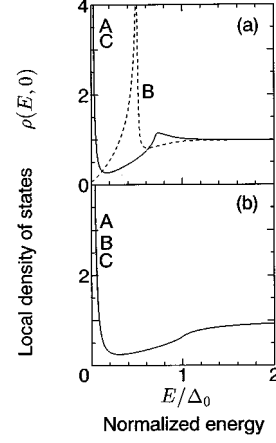
FIG. 13. Normalized local density of states $\rho(E,0)$ is calculated for $\alpha=\pi/4$ and $\beta=0$, with A: $\varphi=0$, B: $\varphi=\pi/2$ and C: $\varphi=\pi$. (a) $\lambda_0 d=0$, (b) $\lambda_0 d=1$, $\kappa=0.1$.

$$\rho_0(\varphi,\alpha+\pi/2,\beta)=\rho_0(\varphi+\pi,\alpha,\beta),\rho_0(\varphi,\alpha,\beta+\pi/2)$$

$$=\rho_0(\varphi+\pi,\alpha,\beta). \qquad (60)$$

In Fig. 14(a), $\rho_0(\varphi,\alpha,\beta)$ is plotted for the $s/I/s$ junction as a reference. In this case, $\rho_0(\varphi,\alpha,\beta)$ is independent of α and β, and is a monotonically increasing function with $\varphi(0<\varphi<\pi)$. If $\lambda_0 d$ becomes finite, the enhancement at $\varphi=\pi$ is drastically reduced and $\rho_0(\varphi,\alpha,\beta)$ vanishes. In the case of the $d/I/d$ junction, $\rho_0(\varphi,\alpha,\beta)$ has two maxima at $\varphi=0$ and $\varphi=\pi$ for $0<\varphi<\pi$ as shown in Figs. 14(b) and 14(c). This property is very different from that of the $s/I/s$ junction. When α and β have the same sign, $\rho_0(0,\alpha,\beta)<\rho_0(\pi,\alpha,\beta)$ is satisfied. On the other hand, when they have different signs, $\rho_0(0,\alpha,\beta)>\rho_0(\pi,\alpha,\beta)$ is expected.

V. DISCUSSIONS AND CONCLUSIONS

In this paper, the basic properties of the local density of states (LDOS) of d-wave superconductors near the interface
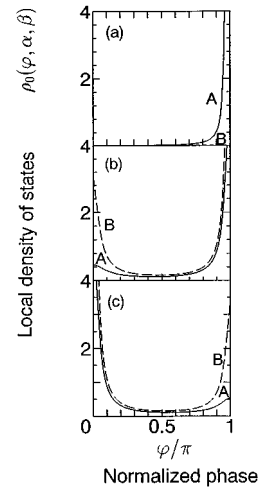
FIG. 14. $\rho_0(\varphi,\alpha,\beta)$ is plotted as the function of φ for various α and β. As a reference $\rho_0(\varphi,\alpha,\beta)$ in a $s/I/s$ junction is plotted in (a). (a) A: $\lambda_0 d=0$, B: $\lambda_0 d=1$, $\kappa=0.5$. In (b) and (c), $\rho_0(\varphi,\alpha,\beta)$ of a $d/I/d$ junction is plotted for various cases with $\lambda_0 d=1$, $\kappa=0.5$. (b) A: $\alpha=0.05\pi$, $\beta=0.1\pi$, B: $\alpha=0.05\pi$, $\beta=0.2\pi$. (c) A: $\alpha=0.05\pi$, $\beta=-0.1\pi$, B: $\alpha=0.05\pi$, $\beta=-0.2\pi$.

is investigated based on the Green's-function method. The LDOS in $N/I/d$ junctions is investigated for various heights and widths of the insulating barrier with changing β, which expresses the angle between the normal to the interface and the crystal axis of the $d_{x^2-y^2}$-wave superconductor. The LDOS has a peak at $E=0$ when the angle between the normal to the interface and the crystal axis of the $d_{x^2-y^2}$-wave superconductor becomes finite, where the transmitted electronlike quasiparticle and holelike quasiparticles from the normal metal feel different signs of the pair potentials. The peak height becomes larger when the magnitude of the height or the width of the barrier increases, and the width of this peak becomes narrower at the same time. The enhancement of the LDOS at $E=0$ is reflected on the tunneling conductances which have been discussed in our previous papers.[22,27] Furthermore, for an infinite thickness or height of the barrier, the LDOS coincides with the previous results of those of semi-infinite d-wave superconductors by Matsumoto and Shiba.[28]

The LDOS at the interface of the $d/I/d$ junction is also investigated. It is revealed that the LDOS strongly depends on the angles, $\alpha(\beta)$ which expresses the angle between the normal to the interface and the crystalline axis of left (right) superconductors and φ, which expresses the macroscopic phase difference between two superconductors. We have obtained generalized expressions of the energy levels of bound states and the LDOS which include several limiting cases. The $\rho_0(\varphi,\alpha,\beta)$, which expresses the φ, α, and β dependences of LDOS at zero energy, shows peculiar behaviors. The important point is that $\rho_0(\varphi,\alpha,\beta)$ is not always a monotonically increasing function of φ for fixed α and β. This fact is very different from that of conventional $s/I/s$ junctions. It is known from the previous investigations of the Josephson effect in $s/I/s$ junctions, that the ZES influence crucially the φ dependence of the Josephson current.[8,11] Since the φ dependence of ZES in $d/I/d$ junctions is much more complex as compared with that of the $s/I/s$ junctions, we can expect an unconventional φ dependence of the Josephson effect. In the Josephson junction including a d-wave superconductor, the Josephson current strongly depends on the direction of the junction. We have clarified in $s/I/d$ junctions, even when the ZES do not exist, the φ dependence of Josephson current is different from that of the conventional Josephson effect.[33,34] Under the existence of ZES, there may be phenomena which cannot be expected in the conventional Josephson effect. For example, there is a possibility that Josephson current is not a monotonically increasing function with the decrease of temperature.[35] The detailed results will be published elsewhere.

There are several experiments which report ZES. Edwards et al.,[36] showed that tunneling into freshly cleaved c-axis surfaces of Y-Ba-Cu-O via scanning tunnel microscopy (STM) gave different results for the density of states, depending on whether the oxygen content in the chain was locally stoichiometric or not. At the sites of oxygen vacancies, the density of states was apparently normal, with a broad zero-energy peak. Hence one might imagine that tunneling into the ab plane would give different results, depending on the local oxygen stoichiometry at the STM site.[36] The magnitude of zero-energy peak is not large as that of in our theories. However, by choosing parameters of barrier and

taking into account the roughness at the interface, the magnitude of the zero-energy peak can be as large as in the experiments. Another possible explanation of zero-energy peaks is due to the role of surface or interface states which originate from the layered structure.[37]

There are several open problems. In this paper, to see the essence of the anisotropy of d-wave superconductors, we assumed a two-dimensional model. Since actual high-T_c cuprates are regarded as two-dimensional superconductors, our two-dimensional model will be valid. In general, we can straightforwardly extend the present theory to three-dimensional cases. In such cases, the detailed features of LDOS is changed. However the essence of physics is not changed, and we can also expect the ZES for several cases. As regards $d_{x^2-y^2}$-wave superconductors, the ZES are formed at the interface for $N/I/d$ or $d/I/d$ junctions with ab-plane contact. On the other hand, we cannot expect the ZES for $N/I/d$ and $d/I/d$ junctions for finite width of the insulator with c-axis orientation. The essential point for the formation of ZES at the interface of superconductor is that a transmitted and a reflected electron(hole) like quasiparticle feel the different signs of the pair potentials (see Fig. 8). It should be emphasized that ZES are generally expected for three-dimensional anisotropic superconductors. So we can expect ZES in heavy fermion superconductors.[38]

With regards to tunneling along the c axis, Katz et al.[39] and Sun et al.[16] observed Josephson current in Y-Ba-Cu-O/Pb junctions. If we assume the symmetry of the pair potential of Y-Ba-Cu-O is $d_{x^2-y^2}$ wave, the obtained Josephson current is proportional to $\sin(2\varphi)$,[33] and the magnitude of Josephson current is drastically reduced which contradicts with observed value. Sigrist et al. proposed that one of the time-reversal symmetry-breaking states, i.e., $s+id$-wave state, is induced at the twin boundary in Y-Ba-Cu-O. In such cases, Josephson coupling is much more enhanced.[40] However, the $s+id$-wave state at twin boundaries as proposed by Sigrist et al. would likely lead to overdamped Fiscke modes in highly twinned Y-Ba-Cu-O/Pb c-axis junctions, contrary to experiments.

In the present paper, the spatial dependence of the pair potentials are assumed to be constant. It has been revealed very recently by Nagato and Nagai,[23] that the spatial dependence of the pair potentials near the interface depends on the angle between the crystalline axis and the normal to the interface. However, the qualitative features of ZES are not changed seriously. In their theory, a model of finite thickness superconductor is employed. We are planning to calculate the pair potentials self-consistently in more general cases, e.g., $N/I/d$ or $d/I/d$ junctions, extending our previous numerical calculations in the s-wave superconductors.[9] Furthermore, the coexistence of another kind of symmetry of pair potentials near the interface is also expected.[41] If the time-reversal symmetry is broken at the interface, the promising states are $s+id_{x^2-y^2}$-wave states or $d_{xy}+id_{x^2-y^2}$-wave states.[42–44] In such a case, the LDOS near the interface is changed, since ZES are not formed at the interface. It is interesting to know how the tunneling conductance and LDOS are influenced by the coexistence of two kinds of pair potentials. It is necessary to solve this problem to clarify several tunneling experiments more quantitatively.

[1] W. L. McMillan, Phys. Rev. B **175**, 559 (1967).

[2] A. F. Andreev, Zh. Eksp. Teor. Fiz. **46**, 1823 (1964) [Sov. Phys. JETP **19**, 1228 (1964)].

[3] I. O. Kulik, Sov. Phys. JETP **30**, 944 (1970).

[4] J. Bardeen and J. L. Johnson, Phys. Rev. B **5**, 72 (1972).

[5] R. Kümmel, Phys. Rev. B **16**, 1979 (1977); R. Kümmel and W. Senftinger, Z. Phys. B **59**, 275 (1985).

[6] T. M. Klapwijk, Physica B **197**, 481 (1994).

[7] C. Ishii, Prog. Theor. Phys. **44**, 1525 (1970); **47**, 1464 (1972).

[8] A. Furusaki and M. Tsukada, Phys. Rev. B **43**, 10 164 (1991).

[9] Y. Tanaka and M. Tsukada, Phys. Rev. B **37**, 5087 (1988); **37**, 5095 (1988); **40**, 4482 (1989); **42**, 2066 (1990); **44**, 7578 (1991); **47**, 287 (1993).

[10] M. Ashida, S. Aoyama, J. Hara, and K. Nagai, Phys. Rev. B **40**, 8673 (1989); M. Ashida, J. Hara, and K. Nagai, *ibid.* **45**, 828 (1992); Y. Nagato and K. Nagai, J. Low Temp. Phys. **93**, 33 (1993); S. Higashitani and K. Nagai, J. Phys. Soc. Jpn. **64**, 549 (1995).

[11] A. Furusaki and M. Tsukada, Solid State Commun. **78**, 299 (1991).

[12] A. Millis, D. Rainer, and J. Sauls, Phys. Rev. B **38**, 4504 (1998).

[13] Chr. Bruder, Phys. Rev. B **41**, 4017 (1990).

[14] B. Ashauer, G. Kieselmann, and D. Rainer, J. Low Temp. Phys. **63**, 349 (1986).

[15] P. Chaudhari and Shawn-Yu Lin, Phys. Rev. Lett. **72**, 1084 (1994).

[16] A. G. Sun, D. A. Gajewski, M. B. Maple, and R. C. Dynes, Phys. Rev. Lett. **72**, 2267 (1994).

[17] Y. Ohashi, J. Phys. Soc. Jpn. **64**, 887 (1995).

[18] D. A. Wollman, D. J. van Harlingen, W. C. Lee, D. M. Ginsberg, and A. J. Leggett, Phys. Rev. Lett. **71**, 2134 (1993); D. A. Wollman, D. J. Van Harlingen, J. Giapintzakis, and D. M. Ginsberg, *ibid.* **74**, 797 (1994); D. J. Van Harlingen, Rev. Mod. Phys. **67**, 515 (1995).

[19] C. C. Tsuei, J. R. Kirtley, C. C. Chi, L. S. Yu-Jahnes, A. Gupta, T. Shaw, J. Z. Sun, and M. B. Ketchen, Phys. Rev. Lett. **73**, 593 (1994).

[20] M. Sigrist and T. M. Rice, J. Phys. Soc. Jpn. **61**, 4283 (1992); Rev. Mod. Phys. **67**, 503 (1995).

[21] A. Mathai, Y. Gim, R. C. Black, A. Amar, and F. C. Wellstood, Phys. Rev. Lett. **74**, 4523 (1995).

[22] Y. Tanaka and S. Kashiwaya, Phys. Rev. Lett. **74**, 3451 (1995).

[23] J. Geerk, X. X. Xi, and G. Linker, Z. Phys. B **73**, 329 (1988).

[24] T. Walsh, Int. J. Mod. Phys. **6**, 125 (1992).

[25] I. Iguchi, Physica C **185−189**, 241 (1991).

[26] S. Kashiwaya, M. Koyanagi, M. Matuda, and K. Kajimura Physica B **194−196**, 2119 (1994).

[27] S. Kashiwaya, Y. Tanaka, H. Takashima, M. Koyanagi, and K. Kajimura, Phys. Rev. B **51**, 1350 (1995).

[28] M. Matsumoto and H. Shiba, J. Phys. Soc. Jpn. **64**, 1703 (1995).

[29] Y. Nagato and K. Nagai, Phys. Rev. B **51**, 16 254 (1995).

[30] C. R. Hu, Phys. Rev. Lett. **72**, 1526 (1994); Jian Yang and C. R. Hu, Phys. Rev. B **50**, 16 766 (1994).

[31] S. Kashiwaya, Y. Tanaka, M. Koyanagi, and K. Kajimura, *Advances in Superconductivity III*, edited by K. Yamafuji and T. Morishita (Springer-Verlag, Tokyo, 1995), p. 45; Jpn. J. Appl. Phys. **34**, 4555 (1995); J. Phys. Chem. Solid **56**, 1721 (1995).

[32] S. Kashiwaya, Y. Tanaka, M. Koyanagi, and K. Kajimura, Phys. Rev. B **53**, 2667 (1996).

[33] Y. Tanaka, Phys. Rev. Lett. **72**, 3871 (1994).

[34] Y. Tanaka, Physica C **235−240**, 3205 (1994).

[35] Y. Tanaka and S. Kashiwaya J. Phys. Chem. Solid **56**, 1761 (1995); Physica C (to be published).

[36] H. L. Edwards, D. J. Derro, A. L. Barr, J. T. Markert, and A. L. de Lozanne, Phys. Rev. Lett. **75**, 1387 (1993).

[37] S. H. Liu and R. A. Klemm, Phys. Rev. B **52**, 9657 (1995).

[38] M. Sigrist and K. Ueda, Rev. Mod. Phys. **63**, 239 (1991).

[39] A. S. Katz, A. G. Sun, R. C. Dynes, and K. Char, Appl. Phys. Lett. **66**, 105 (1995).

[40] M. Sigrist, K. Kuboki, P. A. Lee, A. J. Millis, and T. M. Rice (unpublished).

[41] J. H. Xu, Y. R. Ren, and C. S. Ting, Phys. Rev. B **52**, 7663 (1995).

[42] K. Kuboki and M. Sigrist, J. Phys. Soc. Jpn. (to be published).

[43] M. Matsumoto and H. Shiba, J. Phys. Soc. Jpn. **64**, 3384 (1995); **64**, 4867 (1995).

[44] T. Koyama and M. Tachiki, Phys. Rev. B **53**, 2662 (1996).